Real-Time Microradiography of Pearls: A Comparison Between Detectors

Stefanos Karampelas, Abeer Tawfeeq Al-Alawi, and Ali Al-Attawi

Over the past ten years, gemological laboratories have been replacing film-based microradiography with real-time X-ray microradiography (RTX). This paper compares the output quality and resolution provided by two RTX units fitted with different detectors: an image intensifier (II) and a flat panel detector (FPD) using the same type of X-ray generating tube. Although the II is faster and less expensive, the images acquired with the FPD show greater detail of the pearl's internal growth structures, making interpretation and consequent conclusions easier to validate.

Since the early 20th century, gemological laboratories have been using film-based microradiography to reveal minute structures that separate natural from cultured pearls, sometimes alongside other methods such as Laue diffraction and endoscopy (e.g., Galibourg and Ryziger, 1927; Anderson, 1932; Alexander, 1941; Webster, 1954; Farn, 1980; Hänni, 1983; Poirot and Gonthier, 1998; Scarratt et al., 2000; Sturman, 2009). Today, real-time X-ray microradiography (RTX) is the foremost testing method for carrying out this vital work. It can also be paired with the more time-consuming X-ray computed microtomography for challenging identifications and research purposes (Karampelas et al., 2010; Krzemnicki et al., 2010).

With film-based microradiography, pearls are sometimes placed in direct contact with a high-resolution film cassette or immersed in a scatter-reducing liquid (e.g., lead nitrate solution or carbon tetrachloride, both of which are hazardous). X-ray scattering may also be reduced by simply surrounding individual pearls with a thin lead sheet or film. Regardless of the technique, a darkroom and a series of chemicals are necessary for film processing. It takes approximately 20 minutes to select the film and secure the pearls to the film cassette. At the same time, the exposure must be determined assuming an average-sized sample and keeping in mind that pearls in a strand are often graduated in size and that spheres require longer exposure times through the centers than the edges. Next, the film must be developed, fixed, and dried. All told, it is a time-consuming process.

The last 20 years have seen RTX steadily replace film-based radiography in the medical sector, and over the last decade most gemological laboratories have followed this trend by partially or fully adopting RTX. This method has several important advantages. No hazardous liquids are needed, and it gives immediate or nearly immediate results, which are easier to store and share among a team of technicians or in publications and presentations. RTX microradiography also requires a lower total amount of radiation than film-based microradiography, though similar X-ray generating tubes may be used without a need to reduce X-ray scattering. Some gemological laboratories initially employed RTX units with image intensifier (II) technology generally associated with digital cameras to acquire RTX microradiographs. More recent units have employed flat panel detectors (FPD), which can be of larger dimension with high resolution. However, FPD costs approximately US$25,000, about 40% more than II units and cameras.

An II is a vacuum tube device that converts invisible X-rays transmitted through the sample into visible light by a cesium iodide (CsI) scintillator. The visible light is then converted into electrons at the photoelectric surface and emitted inside the vacuum tube. The emitted electrons are accelerated and focused by electrodes, which act as an electron lens, onto the output screen and converted into bright visible light that is captured by a digital camera (figure 1, left; Ide et al., 2015). On the other hand, an FPD is a thin, flat solid sensor where invisible X-rays transmitted through the sample are converted into visible light, also by a CsI scintillator. The visible light is

See end of article for About the Authors and Acknowledgments.
Gems & Gemology, Vol. 53, No. 4, pp. 452–456,
http://dx.doi.org/10.5741/GEMS.53.4.452

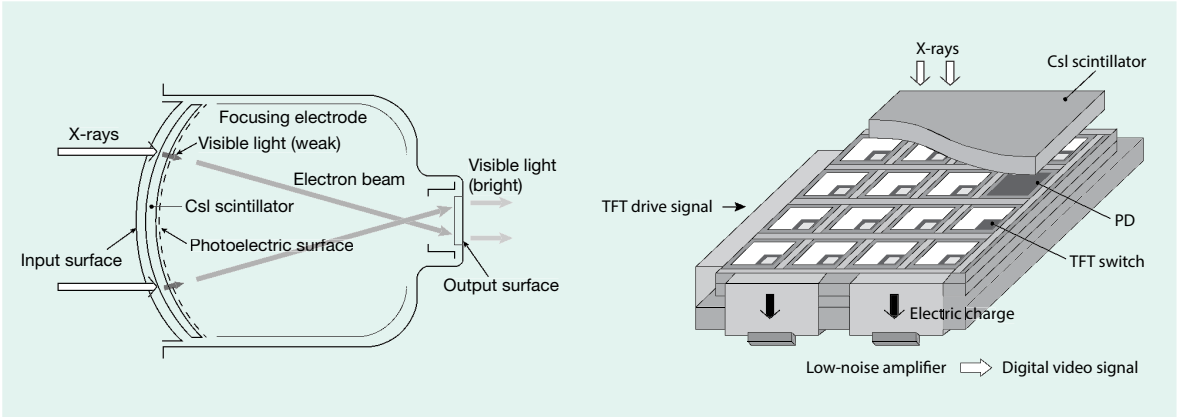

Figure 1. Structures and principles of operation for an II (left) and an FPD (right). Modified after Ide et al. (2015).

converted into an electric charge stored in each photodiode (PD). The signals are read by a thin-film transistor (TFT) switch provided for each pixel and amplified by a low-noise amplifier, undergoing analog-digital conversion to become digital video signals (figure 1, right; Ide et al., 2015).

The quality of the RTX microradiographs depends on the system's resolution (usually given in line pairs per millimeter, or LP/mm), the magnification, and the exported image size. The images are processed and initially viewed with software linked to the instrument or, more commonly, third-party software such as Fiji (ImageJ) or Adobe Photoshop. To view the microradiographs, a relatively large high-resolution screen (>20 inch) should be used. For this study, RTX microradiographs were acquired for the same set of samples (figure 2 and table 1) using the two different systems described above.

MATERIALS AND METHODS

Two undrilled and two drilled samples of various sizes from different mollusks were selected for this study (figure 2 and table 1): one natural saltwater pearl, one bead-cultured saltwater pearl, one non-bead-cultured freshwater pearl, and one non-bead-cultured saltwater pearl.

Microradiographs were acquired at the Bahrain Institute for Pearls and Gemstones (DANAT) using two RTX units: a FocalSpot (San Diego, California) Verifier HR FSX-090 and a Pacific X-Ray Imaging (PXI, San Diego, California) GenX-90. The electronics and imaging systems of both units were provided by PXI. Microradiographic images were collected in the same direction for each sample. Both instruments have the same tube type, a Thermo Scientific PXS5-928 with a spot size of <9 microns. The FocalSpot unit has a Toshiba E5877J-P1 image intensifier (two-inch and

Figure 2. The four samples from this study. Left to right: three cultured pearls (sample numbers 19, 21, and 8) and a natural pearl (sample number 1). The largest sample is 15.65 mm tall. Photo by Ghadeer Abdali, © DANAT.

TABLE 1. General characteristics of saltwater pearl samples.

Sample no.	Type	Mollusk	Size	Shape
1	Natural saltwater	*Pinctada radiata*	5.69–5.75 × 5.00 mm	Button[a]
8	Bead-cultured saltwater	*Pinctada fucata*	5.14 × 5.23 × 5.50 mm	Oval[b]
19	Non-bead-cultured saltwater	*Pinctada maxima*	11.63 × 12.37 × 15.65 mm	Baroque[a]
21	Non-bead-cultured freshwater	*Hyriopsis* species	10.29–10.86 mm	Near-round[b]

[a]*Undrilled*
[b]*Drilled*

four-inch options) with >40 LP/mm resolution at high magnification and a camera with 0.5 MB resolution. Due to the instrument's size and the X-ray tube collimator to minimize distortion, the maximum sensitive area is 33 × 33 mm^2 (with some areas at the corners not active, as an II initial field of view is round). The PXI unit has a Perkin Elmer Dexela 1512 flat panel detector with >40 LP/mm resolution at high magnification, a pixel size of 75 microns, 3072 × 1944 resolution, and a sensitive area of 33 × 33 mm^2, reduced from 49 × 56 mm^2 due to the X-ray tube filter.

In Brief

- Most gemological laboratories have been replacing film radiography with real-time X-ray microradiography (RTX) to separate natural and cultured pearls.
- A comparison of RTX units with image intensifier (II) and flat panel detector (FPD) technology shows that the first is more economical and produces faster results.
- An FPD yields images with less noise and greater detail of a pearl's internal structures, making it more suitable for their characterization.

The maximum frame averaging used to decrease noise was 256 frames for the II and 128 frames for the FPD. X-radiation of 70–90 kV accelerating voltage and 70–90 µA current were used in both instruments with an exposure time of 100–250 milliseconds per frame. The acquisition times for each microradiographic image were approximately 10 seconds for the II and 100 seconds for the FPD. The images were exported as TIF files, with a maximum resolution of 300 KB/8-bit grayscale and 6 MB/16-bit grayscale, respectively. For each sample, microradiographs were taken from three directions perpendicular to each other. The images were manipulated with Fiji (ImageJ) version 1.0 using Java 6, an open-source software.

RESULTS AND DISCUSSIONS

Selected radiographs of all four samples are shown in figures 3–6. Microradiographs acquired with the FPD are provided on the left, while images collected using the II system are on the right. All images are grayscale; lighter tones indicate materials with higher density such as calcium carbonate (usually aragonite for most gem-quality pearls, as in this study), while darker tones represent lower-density materials (usually organic matter, cracks, or cavities/voids). To view

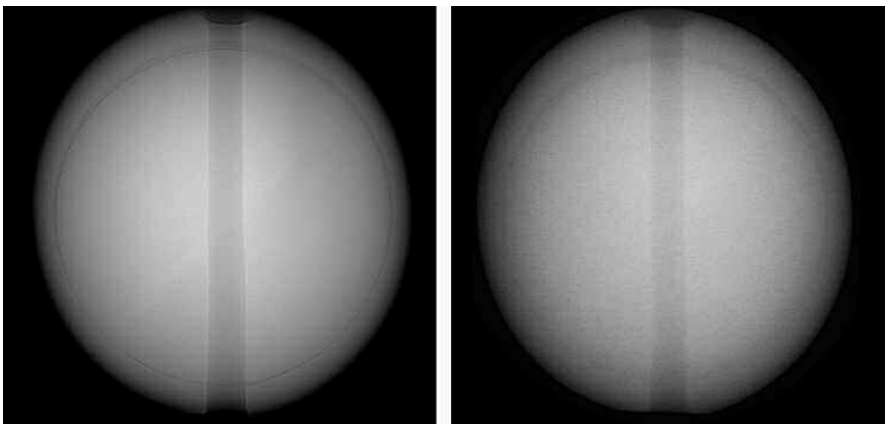

Figure 3. Microradiographs of sample 8, a bead-cultured saltwater pearl from Pinctada fucata, *produced with an FPD (left) and an II (right). The diameter of the bead is about 4.5 mm.*

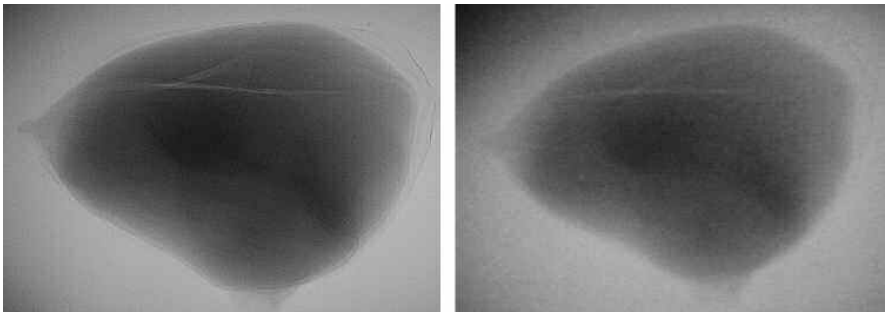

Figure 4. Microradiographs of the center of sample 19 (a non-bead-cultured saltwater pearl from Pinctada maxima*), produced with an FPD (left) and an II (right); fields of view approximately 7 mm.*

the raw original images, visit www.gia.edu/gems-gemology/winter-2017-microradiography-pearls and see supplementary items S3–S6. Figure 3 presents the microradiographs of a bead-cultured saltwater pearl from *Pinctada fucata*. The implanted bead, which presents no structure and is almost centered, is clearly indicated by a dark growth line running inside the edge of the sample and roughly parallel with this edge in both microradiographs. This line, made up mostly of organic material, separates the bead from the nacre overgrowth (Scarratt et al., 2000). The microradiographs acquired with an II appear less clear than those produced with the FPD, which allow the growth line surrounding the bead to be clearly viewed. This feature appears less clear in the II along several parts of the growth line.

Figure 4 presents the magnified microradiographs of the central part of a non-bead-cultured saltwater pearl from *Pinctada maxima*. A large irregular dark gray area that allows this sample to be identified is clearly observed in both microradiographs (Krzemnicki et al., 2010). However, the microradiograph acquired with an FPD reveals additional information in the form of light lines within the dark gray center and growth lines around it.

Figure 5 presents magnified microradiographs of the central part of a natural saltwater pearl from *Pinctada radiata*. Both images reveal an "onion-like" structure with a darker color and a dark spot in the center, a characteristic of natural pearls (Scarratt et al., 2000; Karampelas et al., 2010; Krzemnicki et al., 2010). Additionally, some dark areas and lines are observed toward the outer part of the sample. In the microradiograph acquired with the II, the dark center and the various growth lines are barely visible. It is very noisy, and thus further information cannot be revealed. In the microradiograph produced with an FPD, several additional lines are observed as well as some radial structures in the darker part of the sample. These structures, which likely result from the radial calcite, appear darker due to the enrichment of organic matter that is observed in the center of some natural pearls (Krzemnicki et al., 2010).

In figure 6, ring-like growth structures are recorded in the microradiographs acquired with FPD, as well as a weak, elaborate dark gray area in the center that represents a likely "twisted" cavity-related structure observed in some non-bead freshwater cultured pearls (Scarratt et al., 2000; Sturman, 2009). In the microradiographs acquired with II, fewer and less distinct

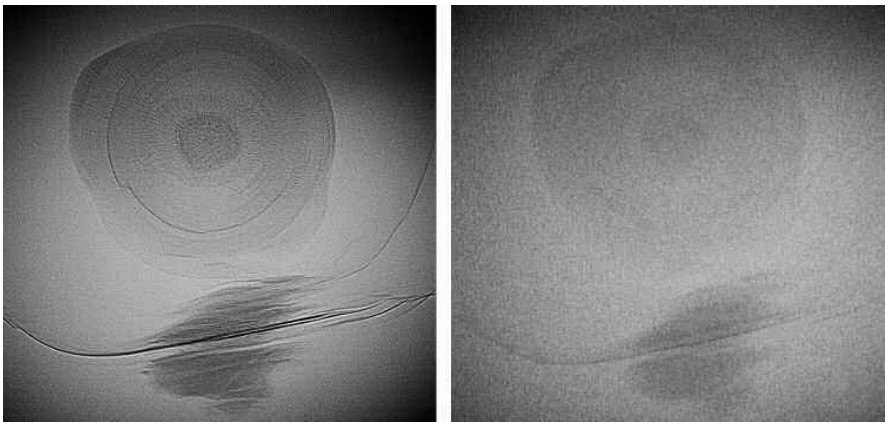

Figure 5. Microradiographs of sample 1 (a natural saltwater pearl from Pinctada radiata*), produced with an FPD (left) and an II (right); fields of view approximately 3.5 mm.*

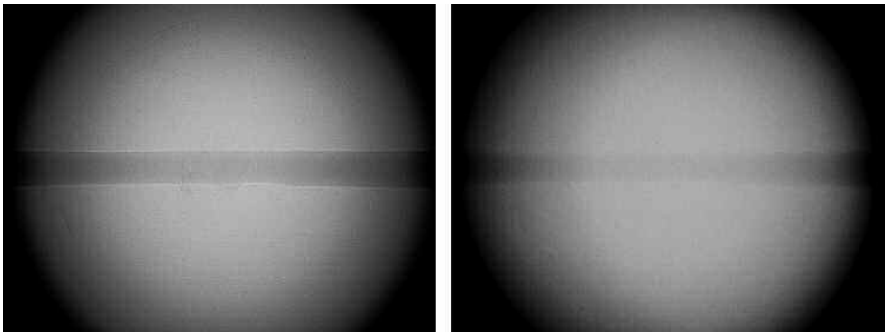

Figure 6. Microradiographs of sample 21 (a non-bead-cultured freshwater pearl from Hyriopsis *species), produced with an FPD (left) and an II (right); fields of view approximately 9 mm.*

growth structures are observed and in the center only a "hair-like" line is barely recorded. Generally, microradiographs of our samples acquired with an II give less distinct images with more noise than those acquired with an FPD; this observation is consistent with previous publications (Baba et al., 2002, 2004).

CONCLUSIONS

RTX microradiography is widely used today by gemological laboratories to separate natural and cultured pearls. Both II and FPD detectors are used for this purpose. An II detector produces faster results than an FPD, and at present the overall cost of an II-based unit is less. On the other hand, FPD images are less noisy and provide greater detail of the internal structures in both natural and cultured pearls, making them more suitable for pearl identification. However, an II could be appropriate for other industries, where the balance between cost and performance is important or when quick response is essential.

ABOUT THE AUTHORS

Dr. Karampelas (stefanos.karampelas@danat.bh) is research director, Ms. Al-Alawi is executive director, and Mr. Al-Attawi is pearl testing manager at the Bahrain Institute of Pearls and Gemstones (DANAT), based in Manama.

ACKNOWLEDGMENTS

The authors thank the gemological team of DANAT for their help with the microradiographs and macro image acquisition. John Donaldson from Pacific X-Ray (PXI) is thanked for the numerous fruitful discussions regarding the specifications sheets of each instrument.

REFERENCES

Alexander A.E. (1941) Natural and cultured pearl differentiation. *G&G*, Vol. 3, No. 12, pp. 184–188.

Anderson B.W. (1932) The use of X-rays in the study of pearls. *The British Journal of Radiology*, Vol. 5, No. 49, pp. 57–64, http://dx.doi.org/10.1259/0007-1285-5-49-57

Baba E., Konno Y., Ueda K., Ikeda S. (2002) Comparison of flat-panel detector and image intensifier detector for cone-beam CT. *Computerized Medical Imaging and Graphics*, Vol. 26, No. 3, pp. 153–158, http://dx.doi.org/10.1016/S0895-6111(02)00008-3

Baba E., Ueda K., Okabe M. (2004) Using a flat-panel detector in high resolution cone beam CT for dental imaging. *Dentomaxillofacial Radiology*, Vol. 33, No. 5, pp. 285–290, http://dx.doi.org/10.1259/dmfr/87440549

Farn A.E. (1980) Notes from the laboratory. *Journal of Gemmology*, Vol. 17, No. 4, pp. 223–229.

Galibourg J., Ryziger F. (1927) Les méthodes d'examen et d'étude des perles fines et des perles de culture. *Revue d'Optique Théorique et Instrumentale*, Vol. 3, pp. 97–133.

Hänni H.A. (1983) The influence of the internal structure of pearls on Lauegrams. *Journal of Gemmology*, Vol. 18, No. 5, pp. 386–400, http://dx.doi.org/10.15506/JoG.1983.18.5.386

Ide H., Yamamoto T., Onihashi H. (2015) X-ray devices contributing to sophistication of X-ray diagnostic systems. *Toshiba Review Edition*, Vol. 1, No. 1, pp. 39–44.

Karampelas S., Michel J., Zheng-Cui M., Schwarz J.-O., Enzmann F., Fritsch E., Leu L., Krzemnicki M.S. (2010) X-ray computed microtomography applied to pearls: Methodology, advantages, and limitations. *G&G*, Vol. 46, No. 2, pp. 122–127, http://dx.doi.org/10.5741/GEMS.46.2.122

Krzemnicki M., Friess D., Chalus P., Hänni H.A., Karampelas S. (2010) X-ray computed microtomography: Distinguishing natural pearls from beaded and non-beaded cultured pearls. *G&G*, Vol. 46, No. 2, pp. 128–134, http://dx.doi.org/10.5741/GEMS.46.2.128

Poirot J.P., Gonthier E. (1998) Le contrôle des perles à partir de 1929 au Laboratoire Gemmologique Français (du laboratoire syndical au laboratoire C.C.I.P.). *Revue de Gemmologie a.f.g.*, Vol. 133, pp. 26–27.

Scarratt K., Moses T.M., Akamatsu S. (2000) Characteristics of nuclei in Chinese freshwater cultured pearls. *G&G*, Vol. 36, No. 2, pp. 98–109, http://dx.doi.org/10.5741/GEMS.36.2.98

Sturman N. (2009) The microradiographic structures on non-bead cultured pearls. www.giathai.net/pdf/The_Microradiographic_structures_in_NBCP.pdf, Nov. 21 [date accessed: Jul. 8, 2017].

Webster R. (1954) Some unusual structures in pearls and cultured pearls. *Journal of Gemmology*, Vol. 4, No. 8, pp. 325–334, http://dx.doi.org/10.15506/JoG.1954.4.8.325